COMPRESSIVE BEHAVIOUR AND FAILURE PATTERNS OF PLAIN AND STEEL FIBER–REINFORCED CONCRETE CYLINDERS UNDER SNI 1974:2011 TEST CONDITIONS

AR Hanung Triyono
Doctor in Environmental, Universitas Semarang, Indonesia. Email: hanungtri@gmail.com

Rezza Ruzuqi*
Politeknik Kelautan dan Perikanan Sorong, Indonesia. Email: rezza.ruzuqi31@gmail.com

Maria Roosa Srah Darmanijati
Institute Teknologi Yogyakarta, Indonesia. Email: darmanijatimaria@gmail.com

Hendro Ahmad Fauzi
Research Center for Structural Strength Technology, National Research and Innovation Agency, Jakarta, Indonesia. Email: hend040@brin.go.id, fins2107@gmail.com

Moch Zaenal Arifin
Bachelor of Civil Engineering, Department of Public Works and Spatial Planning of Central Java Province, Indonesia.

*Corresponding Author: rezza.ruzuqi31@gmail.com

Abstract
Concrete is inherently brittle and prone to crack initiation, which may result in sudden failure under compressive loading. Although compressive strength testing of concrete cylinders in Indonesia has been standardized under SNI 1974:2011, studies systematically applying this standard to evaluate the failure characteristics of steel fiber-reinforced concrete (SFRC) remain limited. This study investigates the effect of hooked-end steel fibers (0.5%, 1.0%, and 1.5% by volume) on the compressive strength and failure behavior of 150 mm × 300 mm concrete cylinders tested in accordance with SNI 1974:2011. The plain concrete specimens exhibited an average compressive strength of 16.84 MPa, characterized predominantly by splitting-type failure. The incorporation of steel fibers increased the average compressive strength to 19.16 MPa, 21.98 MPa, and 29.23 MPa for fiber contents of 0.5%, 1.0%, and 1.5%, respectively. Although the measured strengths remained below the target design strength of fs'45 for pavement concrete, the fiber-reinforced specimens demonstrated cone–shear and shear failure modes with reduced fragmentation and more gradual post-peak behavior. These findings suggest that steel fibers primarily enhance crack control and post-cracking deformation capacity rather than consistently increasing peak compressive strength.

Keywords: Cylindrical Concrete; Compressive Strength; Steel Fiber; Conventional Concrete; SNI 1974:2011

INTRODUCTION

Concrete is the most widely used building material in the world owing to its compressive strength, resistance to several aggressive environmental agents, and economic cost (P Kumar Mehta, 2006). Concrete is, as an example of a complex particulate-based material system, composed of densely packed coarse aggregates and fine aggregates bound by a cementitious binder matrix that fills the voids between the aggregate grains with material binding them together to form a single continuous body.

The practical benefits of concrete in construction: high strength, resistance to fire, corrosion, and aggressive environments have been known for a long while. Furthermore, the formability of concrete to various design geometries offers great flexibility in modern architectural design (Neville & Brooks, 1987). Physically, concrete also undergoes a hydration process: the exothermic reaction of cement with water. This process affects the concrete's final characteristics, particularly when working in aggressive environments. For example, the use of Type II cement can increase resistance to sulfate attack and is particularly suitable for large-scale infrastructure such as bridges and dams (Endawati & Widuri, 2014).

With the increasing importance of concrete durability in recent years, the optimization of hydration has become increasingly crucial; several studies show the need to control hydration more effectively under severe environmental conditions (Zeng et al., 2020). Moreover, the wide availability of raw materials and the low cost of production render concrete a cheap and durable material suitable for a range of construction projects across developed and developing countries. (Darwin et al., 2003)

In line with the growing demands for design innovation and sustainability, concrete technology has also undergone significant advancements. FS 45-grade concrete, for instance, has been widely applied in Indonesian highway projects, including pavement upgrading studies (Hermansyah & Wahidin, 2024), rigid pavement reconstruction (Setiawan & Supratman, 2025), and quality evaluation of rigid pavement layers [8], demonstrating that this grade is representative in both construction practice and research. In this manuscript, FS 45 refers to pavement concrete with a flexural strength (modulus of rupture) of approximately 4.5 MPa (≈ 45 kg/cm²). Based on the mix design guidelines in SNI 03-2834-2000 and the planning practices at the BP2 Laboratory, this value is generally equivalent to structural-grade concrete with a compressive strength of fc' ≈ 35 MPa. To ensure consistency for international readers, this equivalence is denoted as class C35 (fck,cyl ≈ 35 MPa) for terminology alignment—rather than as a formal conversion. (Badan Standardisasi Nasional, 2011; European Committee for Standardization, 2004, 2016; Hunggurami et al., 2017; Kristyanto et al., 2023; National Ready Mixed Concrete Association, 2016)

To address these limitations, a widely investigated approach is steel fiber-reinforced concrete (SFRC). This type of concrete incorporates short, randomly distributed steel fibers throughout the cementitious matrix, which enhances its mechanical properties—particularly its tensile, flexural, and crack resistance. Unlike conventional reinforced concrete, which provides localized reinforcement, steel fibers in SFRC distribute reinforcement uniformly throughout the concrete volume, forming a three-dimensional network that effectively restrains the propagation of micro- to macro-cracks. It has been observed by some researchers that inclusion of steel fibers in medium-strength concrete (C 35) improve post-cracking behaviour and flexural toughness. The study (Koo et al., 2023) investigated concrete strength (EN 14651) higher than 35 MPa and found that when filling was volumetrically increased, more positive residual flexural strengths and ductility were achieved. These results agree with open-access studies (Caballero-Jorna et al., 2021) that have verified the role of fibers and their ability to sustain post-cracking capacity, and with uniaxial compression tests (S.-C. Lee et al., 2015), which demonstrated higher ductility and energy absorption for SFRC. Interestingly, studies on comparative concretes with strengths of 25, 35, and 45 MPa showed that the difference in the post-cracking behaviour between 25 MPa and 35 MPa concretes is quite small, while the concrete with a strength of about 45 MPa tends to have a faster reduction in its post-cracking capacity. This indicates that the C35 class of strength is a suitable range for exploiting the advantages of steel fibers in structural work. The assessment of post-cracking performance in this case is consistent with that proposed by RILEM TC 162-TDF (2003) (STEEL, 2001).

Among the various parameters used to evaluate concrete quality and performance, compressive strength is among the most fundamental. As a result, numerous studies have focused on enhancing concrete's compressive strength, including one that involves incorporating steel fibers. The inclusion of steel fibers has been reported to improve the compressive strength of concrete compared with fiberless mixes (Pour et al., 2021). In high-strength concrete incorporating metakaolin, the inclusion of up to 0.5% steel fibers by volume increased the cylindrical compressive strength by 12.74% (Sharaky et al., 2021). Environmentally friendly high-strength concrete containing recycled steel fibers at a volume fraction of 2% exhibited an 8–12% increase in compressive strength and an improvement in energy absorption capacity of up to 20% (Zhuo et al., 2023). For hollow steel columns filled with high-strength SFRC, the axial compressive capacity increased by 15–18% compared with control columns, accompanied by an ultimate strain increase of up to 25% (Hu et al., 2023).

In civil engineering, the compressive behaviour of concrete is evaluated using standardized test procedures to ensure consistent, comparable results. In Indonesia, this evaluation refers to SNI 1974:2011, which describes the procedure for obtaining the compressive capacity of cylindrical test pieces [21]. Under this standard, cylinders 150 mm in diameter and 300 mm in height are placed in a compression test frame and loaded axially until failure occurs. The nominal compressive stress, fc', is obtained by dividing the peak load recorded during the test by the area of the loaded face of the cylinder. This protocol establishes a standard for judging concrete quality and facilitates comparisons across different studies and field applications.

To provide a comparable quantitative context, Table 1 summarizes the 28-day compressive strength (f'c) values of C35-grade concrete in three configurations—plain concrete, reinforced concrete (RC), and steel fiber-reinforced concrete (SFRC)—based on cylindrical compressive test results reported (Gerges et al., 2023; T. Lee & Lee, 2020; Neves & Fernandes de Almeida, 2005).

Table 1. 28-day compressive strength (f'c) of C35-grade concrete for plain concrete, reinforced concrete (RC), and steel fiber-reinforced concrete (SFRC), based on cylindrical compressive test results from selected literature [22-24]

Type	Characteristics	Age (days)	Compressive Strength (MPa)	Reference

Plain concrete (C35, without fibers)	Normal mix without reinforcement; water–cement ratio ≈ 0.48	28	35.2 ± 1.0	[22]
Reinforced concrete (RC, C35)	RC beam with fc' = 35 MPa (cylindrical specimen Ø150 × 300 mm)	28	35.0	[24]
Steel fiber-reinforced concrete (SFRC, C35)	C35 matrix + hooked-end steel fibers (0–1 vol %)	28	38–42	[23]

In this paper, the effects of steel fiber addition on the compressive response and failure mode of cylindrical C35AC specimens, according to a local Indonesian standard, were investigated. Cylinders 150 mm in diameter and 300 mm in length were tested at 28 days of age using the described loading procedure. Quantitative data from compressive strength tests are interpreted together with visual observations of crack development and failure modes, allowing the role of steel fibers in enhancing post-cracking ductility and stabilizing the failure process of concrete within the SNI 1974:2011 testing regime to be elucidated.

MATERIALS AND METHODS

a. Materials

All materials were selected to comply with Indonesian National Standards to ensure consistency with structural concrete applications, including cement, fine aggregate, coarse aggregate, mixing water, chemical additives, and steel fiber as a reinforcing material. The cement used is Ordinary Portland Cement (OPC) Type I, which meets the requirements of SNI 2049-1:2020 (Badan Standardisasi Nasional, 2020). Fine aggregate is natural sand that has been washed and sieved to remove fine particles and organic materials, with a maximum grain size of 4.75 mm, as determined by sieve analysis according to SNI 8321:2016 (Badan Standardisasi Nasional, 2016). Coarse aggregate is crushed stone with a maximum nominal size of 40 mm that meets the gradation and cleanliness requirements of SNI 8321:2016 (Badan Standardisasi Nasional, 2016). The mixing water was taken from the drinking water source, in accordance with SNI 7974:2018 (Badan Standardisasi Nasional, 2018). So, it does not contain substances that are harmful to hydration and the development of cement and concrete strength. As a chemical admixture, high-range water-reducing (HRWR) was used to increase workability without increasing the water-cement ratio. The steel fibers used were hooked-end type with a length of 60 mm and a diameter of 0.90 mm, resulting in an aspect ratio (l/d) of approximately 67, with a fixed dosage of 20 kg/m³ within the recommended range of 15–25 kg/m³ based on the General Specification for Cement Concrete Pavement with Steel Fibers (Division 5.3(4d)). This category of steel fiber is reported to improve mechanical interlocking with the cement matrix and to provide better resistance to fiber pull-out (Yoo & Banthia, 2016).

b. Methods

Specimen Preparation

In this study, four concrete mixture variations were prepared, including one conventional structural concrete without steel fibers used as the control mixture (fs'45) and three steel fiber–reinforced concrete mixtures (fs'45 Fibersteel) incorporating fiber volume fractions of 0.5%, 1.0%, and 1.5%. The control had no added fiber (0%). The chosen fiber volume fraction range is consistent with previous experimental studies showing that steel fibers at 0.5–1.5% significantly enhanced the mechanical performance without harming the workability of structural concrete (Putra et al., 2020; Song & Hwang, 2004; Yoo & Banthia, 2016). The volume basis (vol. %) is presented in Table 2.

Table 2. Concrete mixture proportions expressed in volume fraction (vol.%)

Mix Code	Cement (vol.%)	Water (vol.%)	Coarse Aggregate (vol.%)	Fine Aggregate (vol.%)	Steel Fiber (vol.%)
FS0	12	18	40	30	0.0
FS0.5	12	18	40	29.5	0.5
FS1.0	12	18	40	29.0	1.0
FS1.5	12	18	40	28.5	1.5

The optimum workability around 20 kg/m³ of steel fibers for most experimental studies and a clear increase in mechanical properties can be achieved in structural concrete reinforced with steel fibers (Guan et al., 2023; Ortíz-Lozano et al., 2022), however in practical applications like concrete pavements and slabs, the added quantity ranges from 20–60 kg/m³ at the expense of mechanical performance and workability (Michels et al., 2012). Thus, in this study, different fiber volume fractions were selected to determine the influence of fiber content on the mechanical behaviour of structural concrete.

The entire concrete mixing process was carried out using the wet-mix method. The components, consisting of cement, fine aggregate, coarse aggregate, water, hooked-end steel fiber (Dramix), and type F (High-Range Water Reducer, HRWR) admixture at a dosage of approximately 0.5% of the total cement weight, were loaded into a mixer with a capacity of 1.5–2.0 m³. After thorough mixing, the concrete mixture was transferred to a transit mixer to maintain homogeneity during transportation. Mixing was carried out for 3–5 minutes until a uniform mixture consistency was achieved. This process was followed for all mix variants to ensure that the concrete used to produce the test specimens was the same for comparison of yield and properties.

The main sample used in this study was concrete specimens with a cylindrical shape measuring 150 mm in diameter and 300 mm in height, whose compressive strength was tested according to SNI 1974:2011 (Badan Standardisasi Nasional, 2011). To ensure the test data were statistically reliable and valid, four test specimens were used for each mix variation.

Test Preparation

The compressive strength test was conducted in accordance with the Indonesian National Standard (SNI 1974:2011) using a digital hydraulic compression testing machine (MATEST) with a maximum load capacity of 1500 kN. All specimens were tested at 28 days of curing to determine the standard compressive strength.

The weight and the actual size of each cylinder specimen were measured using a digital balance and common measuring devices, respectively, prior to testing, to determine the parameters needed for compressive strength prediction. The upper and lower faces were waxed to facilitate even surface flattening and reduce surface roughness. Each sample was then placed vertically and concentrically between the upper and lower platen of the testing machine before axial loading.

Test Execution

The compressive strength test was conducted following the procedures outlined in SNI 1974:2011. Cylindrical specimens with a diameter of 150 mm and a height of 300 mm, which had undergone the curing process, were subjected to continuous axial loading at a rate of 0.15–0.35 MPa/s until failure occurred (Badan Standardisasi Nasional, 2011). The maximum recorded load was then used to calculate the concrete compressive strength.

The compressive strength value (f'c) was calculated using the following equation:

$$f'_c = P/A \quad (1)$$

Where:

f'_c = compressive strength of concrete (MPa)

P = maximum load at failure (N)

A = cross-sectional area of the specimen (mm²), calculated as follows:

$$A = \pi x \left(\frac{d}{2}\right)^2 = \pi x \left(\frac{150}{2}\right)^2 = 17{,}671 \text{ mm}^2 \quad (2)$$

Classification Of Specimen Failure Patterns

In addition to measuring compressive strength, visual observations were conducted to analyze the failure patterns of the concrete specimens after testing. The classification of damage followed the SNI 1974:2011 standard, which categorizes cylindrical concrete failures into several main types, as follows:

Type 1 (Cone) → failure forming a conical shape at one end.

Type 2 (Cone and Shear) → a combination of cone failure and inclined shear cracking.

Type 3 (Splitting) → vertical cracks causing the specimen to split into two parts.

Type 4 (Columnar) → longitudinal cracking while the cylinder remains largely intact.

Type 5 (Shear) → failure dominated by a single inclined shear plane.

These observations were documented for each specimen, and the resulting classifications were used to analyze the relationship between steel fiber addition and the concrete's failure mechanism.

RESULTS AND DISCUSSION

Results

Two types of concrete were tested for compressive strength: fiberless structural concrete (fs'45) and steel fiber-reinforced structural concrete (fs'45 Fibersteel). All test specimens were cast in a cylindrical shape with dimensions of 150 mm in diameter by 300 mm high, and then tested after 28 days of hydration according to SNI 1974:2011, 2011.

Table 3: Summary of Strength and Failure Characteristics of the Concrete Specimens, Compressive Strength Test according to SNI 1974:2011, 2011. Normal concrete specimens (FS0) demonstrated compressive strength values in the range of 16.56 to 16.94 MPa, with an average value of 16.84 ± 0.16 MPa. All normal concrete cylinders exhibited splitting failure.

Table 3. Compressive strength and failure characteristics of concrete specimens tested according to SNI 1974:2011

Concrete Type	FiberVolume Fraction (%)	Specimen Code	Compressive Strength (MPa)	Failure Type	Remarks
Plain Concrete	0	FS0-A	16,651	Splitting	Brittle failure
		FS0-B	16,928	Splitting	—
		FS0-C	16,559	Splitting	—
		FS0-D	16,940	Splitting	—
		Mean ± SD	16.84 ± 0.16	Dominant: Splitting	Sudden failure
SFRC	0.5	FS0.5-A	19,995	Shear + Crack bridging	Improved ductility
		FS0.5-B	18,718	Shear	—
		FS0.5-C	18,991	Shear	—
		FS0.5-D	18,921	Shear	—
		Mean ± SD	19.16 ± 0.57	Mixed mode	—
SFRC	1.0	FS1.0-A	22,556	Cone–Shear	Fiber restraint
		FS1.0-B	21,259	Shear	—
		FS1.0-C	23,301	Cone	—
		FS1.0-D	20,805	Shear	—
		Mean ± SD	21.98 ± 1.15	Transition failure	—
SFRC	1.5	FS1.5-A	33,262	Cone	Ductile response
		FS1.5-B	28,867	Cone–Shear	Fiber bridging
		FS1.5-C	27,234	Shear	—
		FS1.5-D	27,554	Cone–Shear	—
		Mean ± SD	29.23 ± 2.78	Cone dominant	Gradual failure

The compressive strength values for steel fiber (SFRC) reinforced concrete with a fiber volume fraction of 0.5% ranged from 18.72 to 19.99 MPa, with an average of 19.16 ± 0.57 MPa. Crack bridging was mainly localized, and shear dominated the failure mode.

The compressive strength at a fiber volume fraction of 1.0% ranged from 20.81 to 23.30 MPa, with an average of 21.98 ± 1.15 MPa. The identified failure modes were cone, shear, and cone-shear.

The compressive strength values obtained in SFRC with 1.5% steel fiber content were 27.23–33.26 MPa, and the average compressive strength was found as 29.23 ± 2.78 MPa at this level of fibers. Cone–type and cone–shear combinations dominated the failure patterns observed in this group.

Steel fiber-reinforced concrete (SFRC) specimens exhibited compressive strengths ranging from 18.72 to 33.26 MPa, depending on the fiber volume fraction used. The compressive strength of SFRC mixtures exhibited a steady increase relative to that of normal concrete, with the highest value belonging to FS1. 5-A specimen at 33.26 MPa. Testing was conducted for all specimens at 28 days under axial loading, referring to SNI 1974:2011.

Next, Figure 1 shows some representative load-time responses collected for the compressive strength tests. To provide a clearer comparison of the curves, the graphs show representative specimens from each mixture variation, selected based on the highest compressive strength. Figure 1(a) represents a concrete specimen without fiber (0% fiber), while Figures 1(b), 1(c), and 1(d) represent steel fiber reinforced concrete with fiber volume fractions of 0.5%, 1.0%, and 1.5%, respectively.

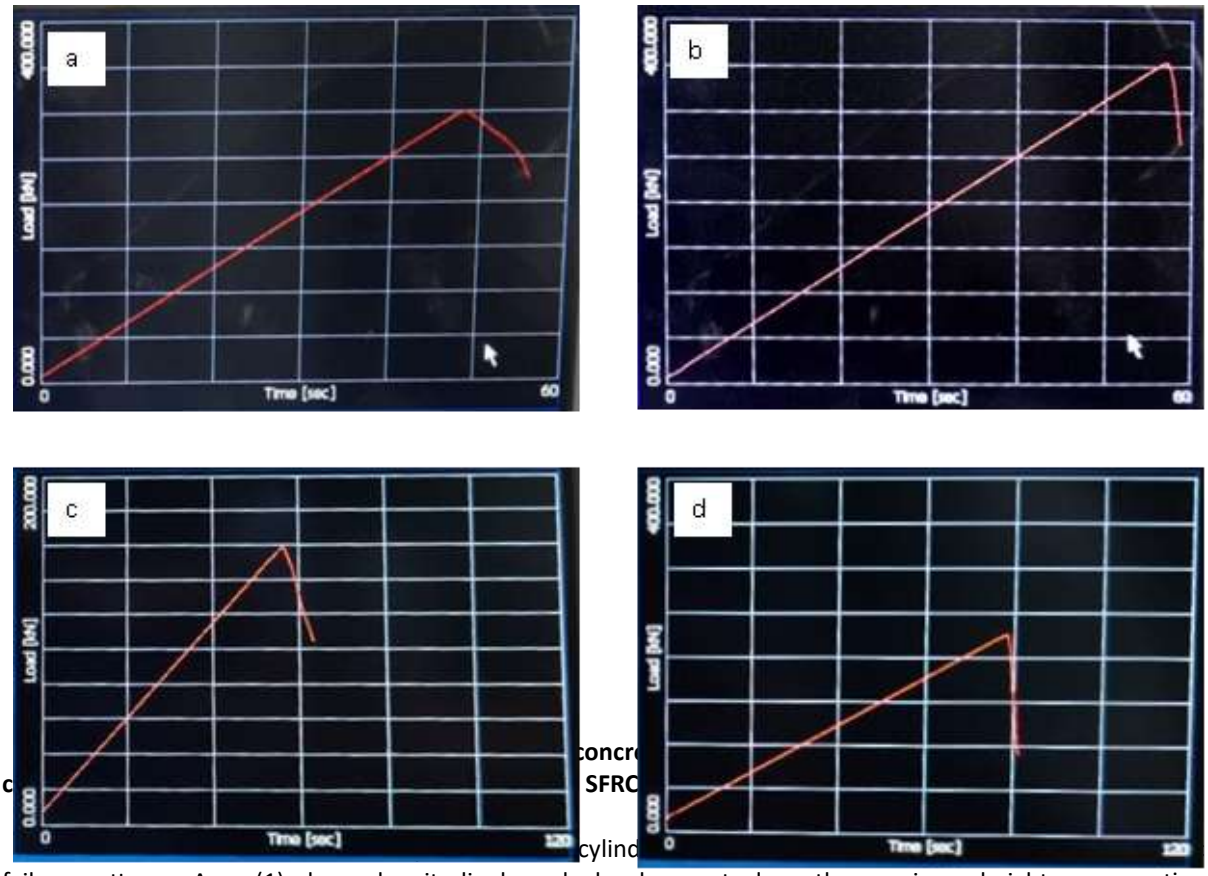

c concr SFRC

cylind

failure patterns. Area (1) shows longitudinal crack development along the specimen height, representing splitting-type deformation prior to reaching maximum failure. Area (2) shows the presence of oblique shear cracks accompanied by local spalling on the concrete surface, while Area (3) exhibits localized crushing damage and exposed aggregate around the loading zone.

Referring to SNI 1974:2011 regarding the classification of failure patterns' sequence, it can be seen that the damage patterns were classified as combined cone-shear and shear failure types. All of the tested concrete cylinders maintained structural integrity after failure, with amplitude-ductile crack propagation over a wide area of the specimen surface.

Fig. 2 Typical compressive failure characteristics of steel fiber–reinforced concrete (fs'45 Fibersteel) specimens: (1) longitudinal cracking, (2) inclined shear cracking with surface spalling, and (3) localized crushing near the loading zone, predominantly exhibiting cone–shear and shear-type failure according to SNI 1974:2011

This shows that for normal concrete specimens (FS0), the compressive strength test results at 28 days are 16.56-16.94 MPa, with an average of 16.84 ± 0.16 MPa, as shown in Table 2. The tests adopted were axial loading of all specimens, in accordance with SNI 1974:2011.

Visual observation of the collapsed concrete cylinders, as shown in Figure 3, demonstrates characteristics of splitting-type failure. Area (1) exhibits dominant longitudinal crack development extending along the specimen's height, while Area (2) exhibits extensive surface spalling accompanied by fragmentation of the concrete after the maximum load is reached. The specimens exhibit clear crack propagation, leading to the separation of the concrete sections along the cylinder's surface.

Based on the failure pattern classification according to SNI 1974:2011, all normal concrete specimens can be categorized as splitting-type failures. After reaching the maximum load, the concrete cylinder fragmented significantly, and several pieces of concrete were found to have been released around the collapsed specimen.

Fig. 3 Typical compressive failure characteristics of plain concrete (fs'45) specimens after axial compression testing, showing dominant longitudinal cracking and surface spalling associated with splitting-type failure according to SNI 1974:2011

Discussion

The results showed that the addition of steel fibers significantly affected the behavior of concrete under axial compressive loading, particularly the failure pattern and post-peak response at 28 days. However, as shown in the results summarized in Table 3, the curve for FS0 (normal concrete without fibers) showed a compressive strength of 16.56-16.94 MPa, with an average of 16.84 ± 0.16 MPa. Meanwhile, steel fiber-reinforced concrete (SFRC) showed an increase in compressive strength with increasing fiber volume fraction, namely 19.16 ± 0.57 MPa (0.5%), 21.98 ± 1.15 MPa (1.0%), and a peak of 29.23 ± 2.78 MPa at 1.5%.

The load response shown in Figure 1 demonstrates that all specimens experienced a relatively linear increase in load until reaching the maximum load. However, the differences became significant after reaching peak condition. A sharp drop of the load without a post-peak tail is observed for concrete with no fibers, and a more gradual drop is observed after reaching peak load with steel fibered concrete. This denotes a replicated behavior, with a limited deformative factor resulting from the integration of steel fibrils within the concrete matrix.

The SFRC specimen in Figure 2 developed rational longitudinal cracks and oblique shear cracks, as well as localized damage around the loading zone. Referring to the failure classification based on SNI 1974:2011, this damage pattern is dominated by combined cone-shear and shear-type failure. Although cracks developed along the specimen surface, the concrete cylinder generally maintained structural continuity after failure. This behavior suggests the presence of a crack-bridging mechanism involving hooked-end steel fibers, which helped restrain crack opening and prevent slippage of the concrete core.

In comparison, normal concrete (Figure 3) has mainly splitting-type failure characteristics. The longitudinal rupture occurred at the cylinder's height, followed by spalling and concrete fragmentation upon reaching the maximum load. The absence of a crack-bridging mechanism caused the concrete fragments to separate rapidly,

resulting in the specimen losing structural continuity and residual bearing capacity immediately after failure. This phenomenon exhibits the brittle behavior of normal concrete under axial compression.

The disparities in strength potential and damage resistance between these two concrete categories are pronounced. FS0 concrete exhibits comparatively low fluctuations in compressive strength but fails abruptly and unstably. In contrast, SFRC has the potential for a broader range of achievable compressive strengths perhaps owing to variable fiber distribution or orientation but it is also much more gradual and presumably more uniform in its failure mechanism. Moreover, the resulting cracks are partially bound by these fibers, which slows down the propagation of damage.

This is extremely useful for elements where stress redistribution or progressive damage occurs, since the system still maintains residual bearing capacity to failure. This observation agrees well with earlier studies that reported that steel fibers increased the toughness of the material by strengthening the interfacial transition zone (ITZ) and delaying the merging of microcracks into unstable macrocracks (Afroughsabet et al., 2016; Johnston, 2014; Yoo & Banthia, 2016).

Further studies can be conducted on other ratios of fiber volume fraction and aspect ratio, or more controlled mixing methods can be used to achieve a more uniform fiber distribution. Additional microstructural characterization using scanning electron microscopy (SEM) or X-ray computed tomography (CT) is also required to measure fiber orientation and crack propagation paths. SNI 1974:2011 test configurations that enable the development of concrete mix designs capable of achieving an adequate balance between compressive strength, post-cracking ductility, and durability for modern structural needs may be used, in addition to Flexure/Cyclic loading or Hybrid Fiber-related tests.

CONCLUSION

This study evaluated the compressive strength and failure characteristics of cylindrical concrete specimens with and without steel fibers, tested in accordance with SNI 1974:2011. The results showed that normal concrete had a compressive strength of 16.56–16.94 MPa, with a relatively consistent splitting failure pattern.

There were progressive increases of the compressive strength with increasing the volume fraction of steel fibers, and they were highest (29.23 MPa) at 1.5% fiber content. Besides enhancing the compressive strength, using steel fibers changed the failure mechanism of concrete when subjected to axial loading. The failure mode of the plain concrete was brittle with remarkable fragmentation after peak load in comparison to concrete with fibers showed a cone-shear and shear type of failure, with adequate structural continuity of the failed specimen. The post-peak behaviour was less abrupt for with steel fibre, indicating a better crack control and energy absorption ability. The crack-bridging mechanism of the steel fibers limited crack propagation, allowing the specimen to retain its residual bearing capacity after reaching the maximum load.

Overall, the main contribution of steel fibers lies not only in increasing compressive strength, but also in increasing damage resistance and post-cracking ductility of concrete. The further developments of this research are to optimal distribution, aspect ratio and hybrid fiber systems on the strength and ductility of RC beams based on establishments with SNI 1974:2011 testing conditions.

Declarations

Author Contributions

Conceptualization, A.H.T.; methodology, A.H.T. and M.R.S.D.; supervision, A.H.T.; validation, A.H.T., H.A.F., and M.Z.A.; data curation, R.R.; formal analysis, R.R., H.A.F., and M.Z.A.; investigation, R.R.; visualization, R.R. and M.Z.A.; resources, M.R.S.D.; project administration, M.R.S.D.; software, M.Z.A.; writing—original draft preparation, R.R.; writing—review and editing, A.H.T., R.R., M.R.S.D., H.A.F., and M.Z.A. All authors have read and agreed to the published version of the manuscript.

Data Availability Statement

Data sharing is not applicable to this article.

Funding and Acknowledgements

The authors extend their sincere appreciation to the Construction Services Center Region IV Surabaya – Directorate General of Construction Development, Ministry of Public Works and Housing (PUPR) for providing the facilities and technical assistance essential for conducting the concrete compressive strength tests. This research was carried out through a collaboration between the Marine and Fisheries Polytechnic of Sorong and Semarang University, whose academic and institutional support is deeply appreciated.

Conflicts of Interest

The authors declare no conflict of interest.

REFERENCES

1. Afroughsabet, V., Biolzi, L., & Ozbakkaloglu, T. (2016). High-performance fiber-reinforced concrete: a review. Journal of Materials Science, 51(14), 6517–6551.
2. Badan Standardisasi Nasional. (2011). SNI 1974:2011: Metode pengujian kuat tekan beton silinder (Standard test method for compressive strength of cylindrical concrete specimens). Badan Standardisasi Nasional.
3. Badan Standardisasi Nasional. (2016). SNI 8321:2016 – Spesifikasi Agregat Beton.
4. Badan Standardisasi Nasional. (2018). Spesifikasi air pencampur untuk produksi beton semen hidraulis (ASTM C1602/C1602M-12, IDT). Badan Standardisasi Nasional .
5. Badan Standardisasi Nasional. (2020). Semen portland - Bagian 1: Spesifikasi SNI 2049-1:2020. Badan Standardisasi Nasional (BSN). https://pesta.bsn.go.id/produk/detail/204912020-sni2049-1:2020
6. Caballero-Jorna, M., Roig-Flores, M., & Serna, P. (2021). A study of the flexural behavior of fiber-reinforced concretes exposed to moderate temperatures. Materials, 14(13), 3522.
7. Darwin, D., Mindess, S., & Young, J. F. (2003). Concrete. Prentice-Hall, Upper Saddle River, NJ.
8. Endawati, J., & Widuri, L. D. D. (2014). Pengaruh Panas Hidrasi Beton Dengan Semen Type II Terhadap Ketebalan Elemen Beton. Jurnal Teknik Sipil Dan Perencanaan, 16(2), 183–194.
9. European Committee for Standardization. (2004). EN 1992-1-1:2004 Eurocode 2: Design of concrete structures—Part 1-1: General rules and rules for buildings. European Committee for Standardization.
10. European Committee for Standardization. (2016). EN 206:2013+A1:2016 Concrete—Specification, performance, production and conformity. European Committee for Standardization. https://doi.org/10.3403/30257890U
11. Gerges, N., Issa, C. A., Sleiman, E., Najjar, M., & Kattouf, A. (2023). Experimental study of the shear behavior of RC beams strengthened with high-performance fiber-reinforced concrete. International Journal of Concrete Structures and Materials, 17(1), 17.
12. Guan, J. L. L., Too, Y. Y., Teh, B. J. W., & Kum, Y. J. (2023). Characterisation of steel fiber reinforced concrete: ductility and service life. Construction, 3(2), 300–307.
13. Hermansyah, J., & Wahidin, W. (2024). ANALISIS STANDAR KUALITAS MATERIAL MUTU BETON FS 45 PADA PEKERJAAN PENINGKATAN JALAN BTS. JABAR-TEGAL–PEMALANG. Infratech Building Journal, 5(1), 1–9.
14. Hu, H.-S., Yang, Z.-J., Xu, L., Zhang, Y.-X., & Gao, Y.-C. (2023). Axial compressive behavior of square concrete-filled steel tube columns with high-strength steel fiber-reinforced concrete. Engineering Structures, 285, 116047.
15. Hunggurami, E., Bolla, M. E., & Messakh, P. (2017). Perbandingan Desain Campuran Beton Normal Menggunakan SNI 03-2834-2000 dan SNI 7656: 2012. Jurnal Teknik Sipil, 6(2), 165–172.
16. Johnston, C. D. (2014). Fiber-reinforced cements and concretes. Crc Press.
17. Koo, D.-H., Kim, J.-S., Kim, S.-H., & Suh, S.-W. (2023). Evaluation of flexural toughness of concrete reinforced with high-performance steel fiber. Materials, 16(20), 6623.
18. Kristyanto, H., Nurokhman, N., & Naufali, D. (2023). Review Mutu Lapisan Beton Fs 45 Pada Ruas Jalan Kokap Kulonprogo. CivETech: Civil Engineering and Technology Journal, 5(2), 10–23.
19. Lee, S.-C., Oh, J.-H., & Cho, J.-Y. (2015). Compressive behavior of fiber-reinforced concrete with end-hooked steel fibers. Materials, 8(4), 1442–1458.
20. Lee, T., & Lee, J. (2020). Evaluation of chloride resistance of early-strength concrete using blended binder and polycarboxylate-based chemical admixture. Applied Sciences, 10(8), 2972.
21. Michels, J., Waldmann, D., Maas, S., & Zürbes, A. (2012). Steel fibers as only reinforcement for flat slab construction–Experimental investigation and design. Construction and Building Materials, 26(1), 145–155.
22. National Ready Mixed Concrete Association. (2016). CIP 16: Flexural strength of concrete. National Ready Mixed Concrete Association.
23. Neves, R. D., & Fernandes de Almeida, J. C. O. (2005). Compressive behaviour of steel fibre reinforced concrete. Structural Concrete, 6(1), 1–8.
24. Neville, A. M., & Brooks, J. J. (1987). Concrete technology (Vol. 438). Longman Scientific & Technical England.
25. Ortíz-Lozano, J. Á., Rodríguez-Narciso, S., Carrillo, J., Hernández-Andrade, J. A., Pacheco-Martínez, J., Hernández-Marín, M., & De La Fuente-Antequera, A. (2022). Mechanical response of industrial concrete with SFRC and PFRC. Advances in Materials Science and Engineering, 2022(1), 8157023.
26. P Kumar Mehta, P. J. M. (2006). Concrete microstructure, properties, and materials. McGraw-hill.

27. Pour, A. F., Ozbakkaloglu, T., & Vincent, T. (2021). Axial compressive behavior of ultra-high-strength steel fiber-reinforced concrete-filled fiber reinforced polymer (FRP) tube columns. Composite Structures, 266, 113777.
28. Putra, A. M., Noorhidana, V. A., & Isneini, M. (2020). Pengaruh penambahan serat baja terhadap kuat lentur balok beton bertulang pada beton mutu normal. Jurnal Rekayasa Sipil Dan Desain, 8(2), 367–384.
29. Setiawan, R., & Supratman, O. (2025). Analisis Perkerasan Kaku (Rigid Pavement) dengan Mutu Beton Fs' 45 terhadap Kuat Tekan dan Lentur: Studi Kasus: Rekonstruksi Ruas Jalan Baros-Petir. Journal of Research and Inovation in Civil Engineering as Applied Science (RIGID), 4(1), 18–26.
30. Sharaky, I. A., Ghoneim, S. S. M., Aziz, B. H. A., & Emara, M. (2021). Experimental and theoretical study on the compressive strength of the high strength concrete incorporating steel fiber and metakaolin. Structures, 31, 57–67.
31. Song, P. S., & Hwang, S. (2004). Mechanical properties of high-strength steel fiber-reinforced concrete. Construction and Building Materials, 18(9), 669–673.
32. STEEL, F. (2001). UNI-AXIAL TENSION TEST FOR STEEL FIBRE REINFORCED CONCRETE. Materials and Structures, 34(1), 3–6.
33. Yoo, D.-Y., & Banthia, N. (2016). Mechanical properties of ultra-high-performance fiber-reinforced concrete: A review. Cement and Concrete Composites, 73, 267–280.
34. Zeng, W., Zhao, Y., Zheng, H., & sun Poon, C. (2020). Improvement in corrosion resistance of recycled aggregate concrete by nano silica suspension modification on recycled aggregates. Cement and Concrete Composites, 106, 103476.
35. Zhuo, K.-X., Cai, Y.-J., Lai, H.-M., Chen, Z.-B., Guo, Y.-C., Chen, G., Xiao, S.-H., & Lan, X.-W. (2023). Axial compressive behavior of environmentally friendly high-strength concrete: Effects of recycled tire steel fiber and rubber powder. Journal of Building Engineering, 76, 107092.